PROCEEDINGS OF SCIENCE

Low Cost Muon Telescope (LOCOMOTE)

Nai-Cheng Huang,[a,*] **Guey-Lin Lin,**[a] **Kwang-Chang Lai,**[b] **M.A. Huang**[c] **and T.C. Liu**[d,e,f,g,h]

[a] *Institute of Physics, National Yang Ming Chiao Tung University, Hsinchu City, Taiwan*
[b] *Center for General Education, Chang Gung University, Taoyuan City, Taiwan*
[c] *Department of Energy Engineering, National United University*
[d] *Department of Electrophysics, National Yang Ming Chiao Tung University, Hsinchu City, Taiwan.*
[e] *Department of applied physics, National PingTung university, PingTung City, Taiwan.*
[f] *Undergraduate Degree Program of Systems Engineering and Technology, National Yang Ming Chiao Tung University, Hsinchu City, Taiwan*
[g] *Chung Cheng Institute of Technology, National Defense University, Taoyuan, Taiwan*
[h] *Leung Center for Cosmology and Particle Astrophysics, National Taiwan University, Taipei, Taiwan*

E-mail: naicheng.Huang55@gmail.com, glin@nycu.edu.tw, kcl@mail.cgu.edu.tw, mahuang@nuu.edu.tw, tcl@nycu.edu.tw

Low Cost Muon Telescope (LOCOMOTE) is a low-cost charged particle detector. Each LOCOMOTE unit includes two pieces of BC408 (2"*2"*1") scintillators, silicon photomultipliers (SiPM), and digital logic circuits. The cost of each LOCOMOTE unit is approximately 200 US dollars and is mainly used as a teaching instrument for high school students in cosmic ray education. Each LOCOMOTE unit can be connected to the network, and data from different units can form a ground array to measure high-energy cosmic ray events. In this report, we present the performance verification of the telescope, including the measurement of cosmic muon angular flux and the feasibility of muon tomography using multiple telescopes.

The 38th International Cosmic Ray Conference (ICRC2023)
Nagoya, Japan
26 July – 3 August, 2023

*Speaker

PoS(ICRC2023)1619

1. Introduction

The Earth is constantly bombarded by cosmic rays. When cosmic rays collide with the nuclei in the atmosphere, they generate extensive cascades of subatomic particles and ionized nuclei, forming an air shower [2]. Within the air shower, only a few kinds of particles (muons and neutrinos) manage to reach the Earth's surface. As neutrinos are challenging to detect due to their extremely small cross section; muons become the primary target for reconstructing cosmic rays by Cherenkov detector on terrain. Muons that reach the Earth's surface are expected to have energy around 4 GeV [6]. By designing affordable and easily expandable muon detector components, we can reduce the cost of students' entry into the field of high-energy research and allow these components to be freely combined for student-designed experiments. This introductory system is named as Low Cost Muon Telescope, LOCOMOTE, as shown by Figure. 1. The components of LOCOMOTE consist of five parts, which include the detection unit with a silicon photomultiplier (SiPM) and scintillator, photomultiplier circuit board, signal processing circuit board, power module, and data system.

The fundamental principle of this detector involves the utilization of the fluorescence effect when atmospheric muons traverse a scintillator [6]. As muons pass through the scintillator, their energy losses are converted into photons. These photons undergo multiple reflections within the scintillator, aided by reflective layers. They are ultimately received by a silicon photomultiplier (SiPM) and transformed into electrical pulses. The signal processing circuit board is employed to determine if signals from multiple channels correspond to the same event.

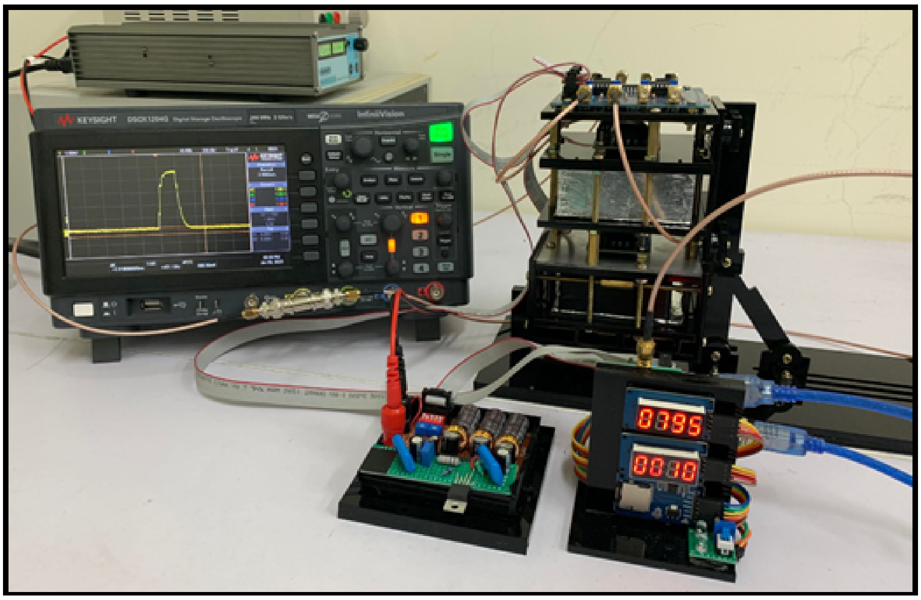

Figure 1: The fundamental LOCOMOTE unit. This unit consists of two sets of SIPM and scintillator detection modules (two channels). Signals from various channels are directed to a coincident circuit for signal interpretation. An event will be recognized as a muon penetration event only when the trigger time difference between the two channels is less than 1 μs.

2. Design and Simulation

2.1 Scintillator detector

Scintillators, such as NaI, CsI, YAG, and LSO, are commonly installed in detectors as charged particle sensors[4]. Hence, scintillators with fluorescent properties are frequently employed in GRB satellite projects or ground-based detectors[6] LOCOMOTE employs BC408 to convert the energy loss of charged particles passing through into photons (Figure.2.(a)). When charged particles traverse the scintillator, their energy loss excites atoms in the material and releases photons. These fluorescent photons are isotropic and propagate within the scintillator. Therefore, the surface of the scintillator needs to be covered or coated with a reflective layer to reflect the photons, in the LOCOMOTE project, low-cost aluminum foil is used as a replacement for expensive reflective films. After multiple reflections, the photons are collected by silicon photomultiplier placed on the scintillator's surface and converted into pulse signals (Figure.2.(b)). By analyzing the waveform of these pulse signals, the energy loss of the charged particles can be calculated, and their type, trajectory, and other characteristics can be determined.

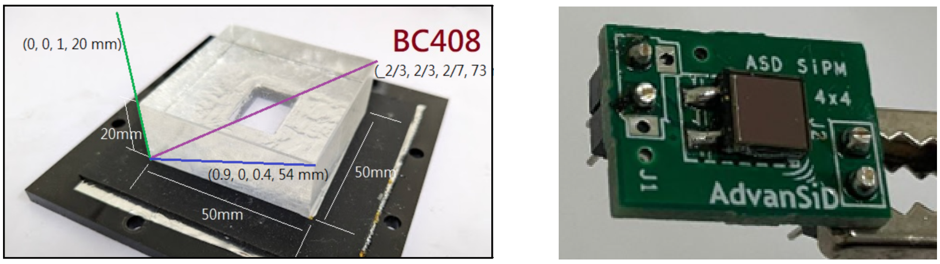

(a) BC408 scintillators

(b) Silicon photomultiplier

Figure 2: (a). BC408 scintillators in LOCOMOTE. BC408 as the material for converting charged particles to light signals. (b).The silicon photomultiplier (SiPM) features small size and high gain, serving as the component in detectors responsible for collecting photons emitted by scintillators (BC408).

2.2 Silicon photomultiplie circuit

The NUV-SiPM utilized in the LOCOMOTE project produces a voltage signal that exhibits clear voltage differences, which can be distinguished by subsequent circuits without amplification. Additionally, the use of high-speed amplifiers can introduce noise, thereby increasing the difficulty of signal interpretation. Consequently, amplifiers are not incorporated into the LOCOMOTE silicon photomultiplier circuit [5][1].

A capacitance value of 0.1 μF is chosen to achieve a pulse width of approximately 1 μs to 2 μs, which is well-suited for subsequent signal processing. However, for applications requiring a significantly higher sample rate within a given time frame, different from typical muon detection, the capacitance value can be adjusted to modify the output signal width. For example, replacing the capacitance with 10 nF will result in a pulse width of 100-200 ns, as illustrated in the output signal reference Figure. 3.(b).

To ensure that the output signal sufficiently drives subsequent circuits and to prevent confusion with environmental noise, we have integrated an offset and voltage stabilization circuit. The comprehensive circuit diagram is available in Figure. 3.(a).

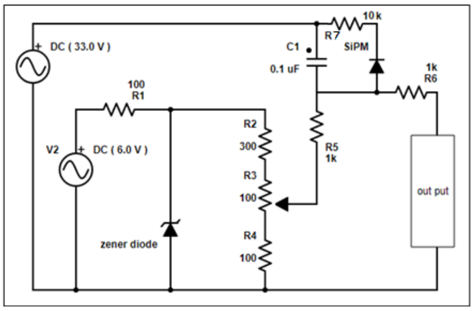

(a) SiPM circuit with offset design

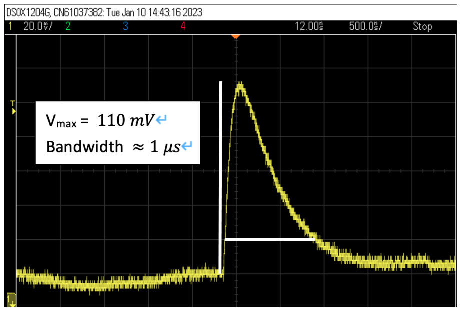

(b) SiPM output pulse

Figure 3: The properties of output signal and SiPM circuit design

2.3 Signal processing board (SPB)

The signal processing board (SPB) of LOCOMOTE integrates the Analog-to-Digital Converter (ADC) and coincidence circuit. The SPB selects the LM319N comparator with a delay of approximately 100 ns to form the ADC. Figure. 4.(a) shows the ADC circuit of SPB. When SiPM output the signal to the SPB as input signal, the width of the output digital signal from SPB is approximately 1 μs. The SPB's coincidence circuit determines if digital signals from different channels overlap to identify coincidental events. In other words, a high-level output signal (coincidental event) is only produced when both channels input high voltage. The output signal can be referred to in Figure. 4.(b).

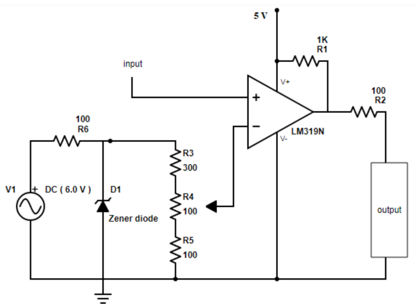

(a) ADC of SPB

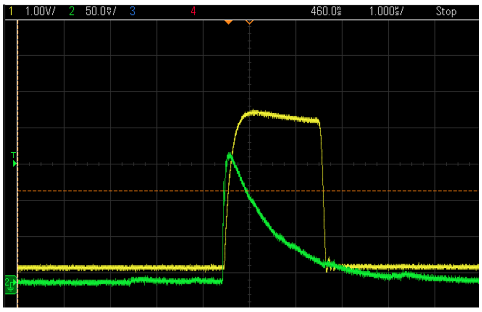

(b) Output of coincidence circuit of SPB.

Figure 4: The signal processing board of LOCOMOTE.

2.4 Detection unit structure and the Field of View

The mechanical structure of LOCOMOTE (shown in Figure 5) is constructed using acrylic and screws. The selection of acrylic is based on its cost-effectiveness, ease of processing, and smaller

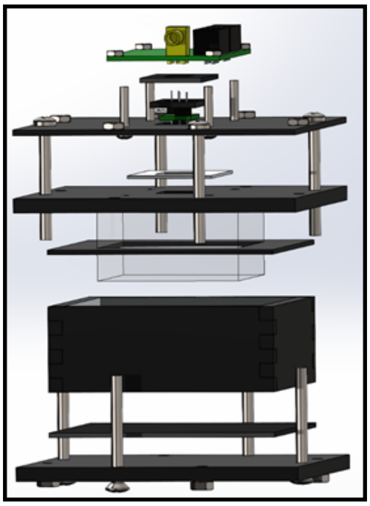

Figure 5: Detector structure explosion diagram. We use acrylic, aluminum foil and oil-resistant pads to complete the light-isolated detection unit.

spacing (cm)	FOV (sr cm^2)
0	144.86 ± 0.39
4	21.33 ± 0.28
8	7.59 ± 0.15
12	3.766 ± 0.081
16	2.24 ± 0.049
20	1.465 ± 0.027
24	1.030 ± 0.025
28	0.764 ± 0.020
32	0.584 ± 0.014
36	0.4647 ± 0.0099

Table 1: The relation between the spacing and FOV.

slant depth compared to metal. LOCOMOTE has the capability to modify the spacing between scintillator modules by adjusting the length of the supporting screws. This alteration in scintillator module spacing can result in a change to the Field of View (FOV) of LOCOMOTE. The relation between the spacing and FOV is shown as Table.1.

2.5 Muon flux simulations and experiments

The flux distribution of muon at the Earth's surface depends on the zenith angle, with a approximately relationship of $F_\mu \propto \cos^2\theta$. By measuring the muon flux using LOCOMOTE and comparing its results to theoretical values, we can verify and calibrate the performance of the LOCOMOTE detector.

This study introduces the modified Gaisser muon formula to estimate the distribution of muon flux at sea level [3] (Figure. 6). The estimated muon flux is incorporated into LOCOMOTE's FOV (Figure. 7), and using the Monte Carlo method, the expected muon flux values that should be measured by the detector at various zenith angles are calculated.

LOCOMOTE measured the atmospheric muon flux in an unobstructed open area (24°47'N, 120°59'E) when facing zenith angles of 0°, 20°, 40°, 60°, and 88°. The measurement result is smaller than the theoretical value, and it is assumed that it is caused by the detection efficiency, which will lose a certain percent of the events; therefore, the ratio of the experimental value and the theoretical value when the detector is facing the zenith angle of 0 degrees is set as the detection efficiency factor, and this is used to do the normalization of the data (Figure. 8), and then after the normalization, the angular distribution of the theoretical and the experimental values are the same, and we believe that the detector does measure the muon.

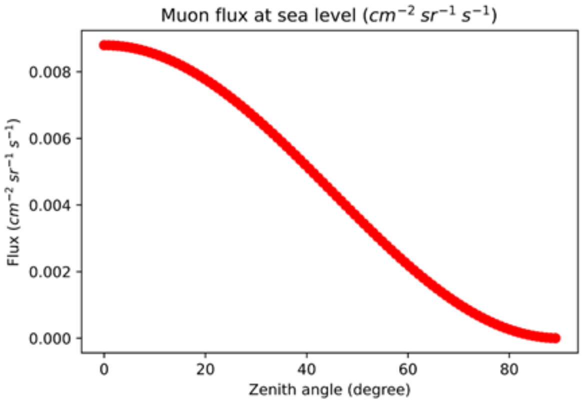

Figure 6: Estimated muon flux at sea level.

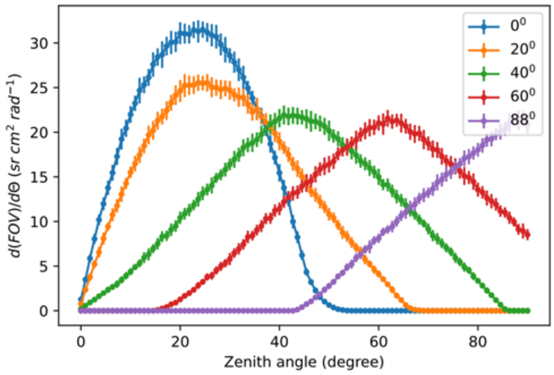

Figure 7: The relationship between field of view of detector and incident angle.

3. Conclusion

The prototype of the two-channel LOCOMOTE demonstrates excellent versatility. In this study, we present LOCOMOTE's measurement of angle-dependent atmospheric muon flux, and the obtained results are consistent with theoretical predictions. Our next step involves making LOCOMOTE available to secondary schools as an elective course to learn about cosmic rays. When the remotely deployed LOCOMOTE units are integrated with GPS-based time sampling and the data is allowed to upload to the cosmic ray server's database, they can also function as a simple ground array. Additionally, the cost-effective modular design of LOCOMOTE's Signal Processing Board (SPB) provides the potential for expansion with more channels. Therefore, we also foresee the potential for this module to serve as a straightforward muon tomography detector. As a result, our upcoming plan includes establishing a 16x16 array of channels for LOCOMOTE to observe the profile of a volcano near Taipei.

4. Acknowledgement

This work is supported by the National Science Councilof Taiwan under Grants 111-2112-M-A49 -013 -MY3.

References

[1] AdvanSiD. URL: https://indico.cern.ch/event/566138/contributions/2287560/attachments/1400219/2139198/Advansid_datasheet_NUV.pdf.

[2] P Auger et al. "Extensive Cosmic-Ray Showers". In: *Reviews of Modern Physics, vol. 11, Issue 3-4, p.288-291* (1939).

[3] M. Guan et al. "A parametrization of the cosmic-ray muon flux at sea-level". In: *arXiv:1509.06176 [hep-ex]* (2015).

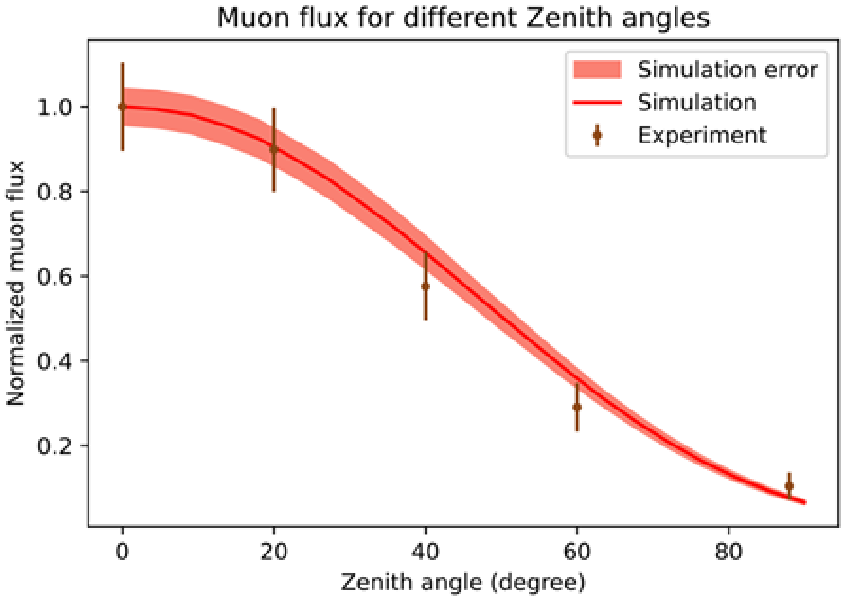

Figure 8: The relationship between atmospheric muon flux and incident angle. The brown data points in this graph represent the actual data obtained from measurements using LOCOMOTE, while the red line represents the theoretical values calculated using the Mengyun Guan approximation equation. In this experiment, LOCOMOTE measured the atmospheric muon flux at different angles starting from a zenith angle of zero. The actual measurement results follow the theoretical angular distribution.

[4] Francesco Maddalena et al. "Inorganic, Organic, and Perovskite Halides with Nanotechnology for High–Light Yield X- and -ray Scintillators". In: *Crystals* 9.2 (2019). ISSN: 2073-4352. DOI: 10.3390/cryst9020088. URL: https://www.mdpi.com/2073-4352/9/2/88.

[5] PhysicsOpenLab. *Front-end electronic for SiPM*. URL: https://physicsopenlab.org/2017/11/28/front-end-electronics-for-sipm/.

[6] R. L. Workman et al. "Review of Particle Physics". In: *PTEP* 2022 (2022), p. 083C01. DOI: 10.1093/ptep/ptac097.